

Sliding Mode Control of a Cable-driven Robot via Double-Integrator Sliding Surface

Alireza Alikhani¹⁺, Mehdi Vali²

¹ Aerospace Research Institute, Tehran, Iran

² Faculty of Engineering, University of Kashan, Kashan, Iran

Abstract. In this paper, robust control of a large cable-driven robot is presented (LCDR). In this mechanism, the cable arrangement eliminates the rotational motions leaving the moving platform with three translational motions. The mechanism has potentials for large scale manipulation and robotics in harsh environments. In this case study, sliding mode control via double integrator sliding surface is presented for tracking control of the robot against inevitable uncertainties. Double-integral sliding mode surface (PIID) is introduced to sliding mode controller to suppress the steady state error in comparison with traditional one. Moreover, there is a common constraint on a LCDR making control problem more challenging. Since cables can only pull the end-effector, control algorithm must ensure all cable tensions are always positive. The asymptotic stability and robustness of the derived control law is proved using direct method of Lyapunov. Finally, the effectiveness of the proposed robust control scheme is demonstrated through simulations.

Keywords: Robustness, sliding mode control, PIID sliding surface, cable-driven robot.

1. Introduction

Cable-driven robots are categorized as a type of parallel manipulators that has recently attracted interests for large scale manipulation tasks. Cable robots are relatively simple in form, with multiple cables attached to a mobile platform or end-effector. The end-effector is manipulated by motors that can extend or retract the cables. A typical cable manipulator requires at least six or seven active cables to restrain all six DoF of the moving platform. However, in most of the applications, a reduced DoF manipulator is sufficient. Behzadipour [1], Notash [2], and Ning [3] presented cable-driven mechanisms with reduced DoF.

In [4], a reduced DoF cable-driven manipulator is introduced similar to BetaBot in [1]. In BetaBot, in order to maintain tension in the cables, a collapsible element called “spine” is used that pushes the end-effector (moving platform) against the robot’s base. In LCDR, however, this role is played by a set of three cables. LCDR has three pure translational motions. In [4], an analytical description for the tensionable workspace of the robot is also found. In [5], kinematics, dynamics and control of LCDR are presented. In this work, a PID-Computed torque control scheme is introduced for trajectory tracking of end-effector. This controller is just robust against step function disturbances and it does not indicate an acceptable performance of the trajectory tracking in the presence of time variant disturbances and unknown model uncertainties. Moreover, In [6], a constrained controller based on traditional sliding mode is developed for control of a modified LCDR with reduced cables. The practical usage of this controller is recognized usually limited as a result of the presence of steady state error in the set-point control of the end-effector.

In this paper, a new robust sliding mode controller is developed in order to tracking control of the end-effector at the presence of unknown but bounded disturbances. Furthermore, it has been broadly known that steady state error of closed-loop system can be effectively suppressed by using of an additional integrator term of the state variables [7]. Thus, steady state error of tracking control of end-effector is going to be

⁺ Corresponding author. Tel.: + (982188366030); fax: +(982188362011).
E-mail address: (roboali@gmail.com).

reduced by adding double integrators to the traditional sliding surface. The asymptotic stability and robustness of the proposed control law is proved using direct method of Lyapunov. Finally, it is important to note, since cables must only pull the end-effector, the control law must ensure all cable tensions are always positive.

The rest of this paper is organized as follow. Section 2 describes the structure of LCDR, followed by its kinematics and dynamic modeling which are presented in Sections 3 and 4 respectively. Control of this manipulator is then presented in Section 5 and Simulation results of position control are given in Section 6. Finally, some conclusions are made in section 7.

2. Structure of LCDR

In Figure 1, a schematic design of LCDR is shown. The middle triangle is the moving platform and the lower and upper triangles are the bases. Three pairs of parallel cables are attached to the moving platform and collected by three spools mounted on the upper base after passing through guide holes on the spool's frames. The spool's shafts are connected to motors (not shown in the figure) to change the length of cables. The spools and their frames are attached to the base, and their configurations with cables and moving platform form three parallelograms. The lower cable driven subsystem which consists of three cables and the corresponding motorized spools, is used to maintain tension in the upper cables.

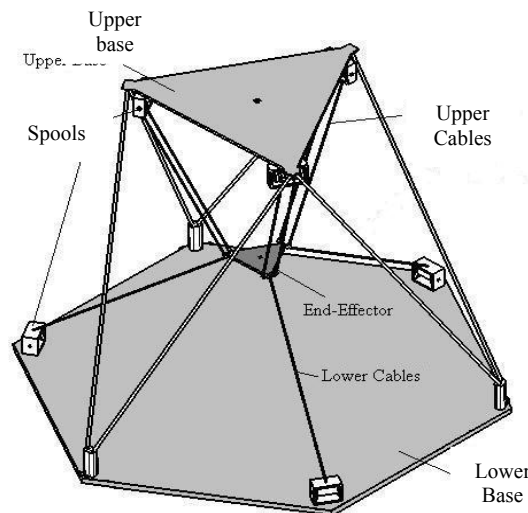


Fig. 1: The General Structure of LCDR.

The equivalent rigid link manipulator for LCDR is analogous to Delta robot [8] and hence can be shown to provide three translational motions for the moving platform. Therefore, it can be concluded that the upper portion of LCDR provides three pure translational motions as long as all cables are in tension.

It is clear that, due to the non-rotating motion of the moving platform there is no possibility of any interference between the cables.

3. Kinematics Modeling

A full development of the kinematics and dynamic equations can be found in [5]. Only an outline of the development, with the final results, is given here.

The kinematics model relates the Cartesian position of the tool frame, mounted on the moving platform, to the variable cable lengths. Figure 2 shows a diagram of the LCDR robot. As seen in the figure, due to the equal cable lengths in each parallelogram, each pair of parallel cables can be replaced by one cable only for the sake of kinematics analysis and therefore, the number of the independent upper cables will be reduced from 6 to 3. And moving platform is considered as a triangle whose vertices are P_1, P_2 and P_3 . The cable vectors of the 6 cables are shown by $\mathbf{L}_i, i=1, 2, \dots, 6$ and the cable lengths are shown by L_i . $\hat{\mathbf{E}}_i$ is a unit vector and represents the direction of the i th cable pointing towards the moving platform.

The inverse kinematic problem is stated as follows: Given the desired position for the centre of the moving platform, \mathbf{P}_m , calculates the cable lengths, i.e. three upper cables and three lower ones.

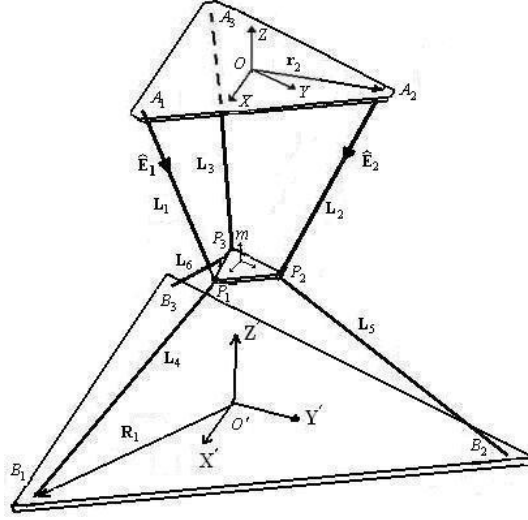


Fig.2: Kinematics Diagram

For upper cables, this can be done by finding the Euclidean norm of the appropriate vectors that represent the upper cables in the Cartesian space:

$$L_i = \left\| \overrightarrow{O'O} + \mathbf{P}_m + \mathbf{c}_i - \mathbf{R}_i \right\| \quad i=1, 2, 3 \quad (1)$$

$\overrightarrow{O'O}$ is the position of frame $\{O\}$ with respect to the origin of $\{O'\}$, expressed in $\{O\}$. Eq. (1) provides an explicit solution for the inverse kinematics.

4. Dynamic Modeling

This section presents the dynamic equations of motion for LCDR. These equations will be used later to ensure that the cable tensions remain positive during the robot operation. Similar analysis on other cable-driven manipulators can be found in [9] and [10]. Here, we assume that the mass and compliance of the cables are negligible and therefore modelled by mass-less slender bars. Also the friction losses between cables and pulleys assumed negligible. Furthermore, our model does not include the actuator dynamics.

The dynamic equation under unwanted disturbances for the moving platform is given by

$$\mathbf{M}\ddot{\mathbf{X}} + \mathbf{G}(\mathbf{X}) = \mathbf{J}\mathbf{t} + \mathbf{D} \quad (2)$$

where $\mathbf{M} = \begin{bmatrix} m_e I_{3 \times 3} & 0_{3 \times 3} \\ 0_{3 \times 3} & 0_{3 \times 3} \end{bmatrix}$ is the inertial matrix, $\mathbf{G}(\mathbf{X}) = \begin{bmatrix} m_e \mathbf{g} \\ \mathbf{r}_g \times m_e \mathbf{g} \end{bmatrix}$ represents the gravitational force,

$\mathbf{t} = [t_1 \ t_2 \ \dots \ t_9]^T$ is the vector of the cable tensions and matrix \mathbf{J} expressed in $\{O\}$ is

$$\mathbf{J} = \begin{bmatrix} \hat{\mathbf{E}}_1 & \hat{\mathbf{E}}_1 & \hat{\mathbf{E}}_3 & \dots & \hat{\mathbf{E}}_5 & \hat{\mathbf{E}}_7 & \hat{\mathbf{E}}_8 & \hat{\mathbf{E}}_9 \\ \mathbf{c}'_1 \times \hat{\mathbf{E}}_1 & \mathbf{c}'_2 \times \hat{\mathbf{E}}_1 & \mathbf{c}'_3 \times \hat{\mathbf{E}}_3 & \dots & \mathbf{c}'_6 \times \hat{\mathbf{E}}_5 & \mathbf{c}'_7 \times \hat{\mathbf{E}}_7 & \mathbf{c}'_8 \times \hat{\mathbf{E}}_8 & \mathbf{c}'_9 \times \hat{\mathbf{E}}_9 \end{bmatrix} \quad (3)$$

Note \mathbf{c}'_i 's are constant vectors determined by the geometry of the moving platform and $\hat{\mathbf{E}}_i$'s are dependent on the position of the moving platform and hence obtained from kinematics. And m_e is the mass, \mathbf{g} is the acceleration vector due to gravity. and $\mathbf{D} = [d_1, d_2, \dots, d_6]^T$ is an unknown but bounded disturbance vector on the end-effector while $|d_i| \leq f_i$ for $i=1, 2, \dots, 6$.

It should be noted here that the equations of motion are valid only if $\mathbf{t} \geq 0$, which means the cables must be all in tension.

5. Double-integrator Sliding mode control

In this section, a robust sliding mode controller is proposed to the LCDR robot (2) for tracking control of the end-effector against unknown disturbances to achieve uniform asymptotically stability along with suppression of the steady state error. As noted previously, since the cables can only pull the end-effector but not push it, the feedback control of suspended cable robots is more challenging. In other words, a suitable

control scheme for a cable-driven robot must not only ensures that the end-effector tracks the desired reference trajectory, but it also guarantees that all cable tensions always maintain positive values.

In sliding mode control, the variable control systems are designed to drive and then constrain the system stable to lie within a neighbourhood of the switching function. The robust sliding mode control design approach consists of two components. The first involves the design of a switching function so that the sliding motion satisfies design specifications. The second is concerned with the selection of a control law which will make the switching function attractive to the system state [11]-[12].

In order to maintain the end-effector to track desired trajectory X_d in the presence of unknown but bounded disturbances and also eliminate the steady state error, the PIID sliding surface is defined as

$$S(X, t) = \ddot{\tilde{X}} + \Lambda_1 \dot{\tilde{X}} + \Lambda_2 \int \tilde{X} dt + \Lambda_3 \int (\int \tilde{X} dt) dt \quad (4)$$

where $S = [s_1, \dots, s_6]^T$, $\tilde{X} = X - X_d$ is defined as tracking error, and Λ_1, Λ_2 and Λ_3 are positive definite constant matrix to be selected i.e. $\Lambda_i = \text{diag}\{\lambda_{i1}, \dots, \lambda_{i6}\}$. To ensure the state of the system approaches the sliding surface, first derivative of the sliding surface should be converged to zero as follow

$$\begin{aligned} \dot{S} &= \ddot{\tilde{X}} + \Lambda_1 \dot{\tilde{X}} + \Lambda_2 \tilde{X} + \Lambda_3 \int \tilde{X} dt \\ &= \mathbf{M}^{-1}[\mathbf{J}\mathbf{t} - \mathbf{G}(X) + \mathbf{D}] - \ddot{X}_d + \Lambda_1(\dot{X} - \dot{X}_d) + \Lambda_2(X - X_d) + \Lambda_3 \int (X - X_d) dt = \mathbf{0} \end{aligned} \quad (5)$$

Approximation of continuous equivalent control law that would achieve $\dot{S} = 0$ may be expressed as

$$(\mathbf{J}\mathbf{t})_{eq} = \mathbf{G}(X) + \mathbf{M}\ddot{X}_d - \mathbf{M}\Lambda_1\dot{\tilde{X}} - \mathbf{M}\Lambda_2\tilde{X} - \mathbf{M}\Lambda_3 \int \tilde{X} dt \quad (6)$$

In order to satisfy sliding condition [11] despite unknown disturbances on the end-effector, a discontinuous term across the sliding surface is added to $(\mathbf{J}\mathbf{t})_{eq}$. Consequently, robust sliding mode control law is proposed as

$$\mathbf{J}\mathbf{t} = (\mathbf{J}\mathbf{t})_{eq} - \mathbf{M}\mathbf{K} \text{sign}(S) \quad (7)$$

where $\text{sign}(S) = [\text{sign}(s_1), \dots, \text{sign}(s_6)]^T$ and K is a positive definite constant matrix i.e. $K = \text{diag}\{k_1, \dots, k_6\}$ depending on upper bound of unknown disturbance and reaching time t_s . Its diagonal elements are selected under following condition.

$$k_i = \sum_{j=1}^6 |(\mathbf{M}^{-1})_{ij}| f_j + \eta_i \quad \text{for } i = 1, \dots, 6 \quad (8)$$

where f_j for $j = 1, \dots, 6$ is upper known bound on disturbance d_j and η_i for $i = 1, \dots, 6$ is strictly positive constant [13].

Finally, the control input (cable tensions) is derived as

$$\mathbf{t} = \mathbf{J}^+ \left[\mathbf{G}(X) + \mathbf{M}\ddot{X}_d - \mathbf{M}\Lambda_1\dot{\tilde{X}} - \mathbf{M}\Lambda_2\tilde{X} - \mathbf{M}\Lambda_3 \int \tilde{X} dt - \mathbf{M}\mathbf{K}\text{sign}(S) \right] + \mathbf{N}(\mathbf{J})\mathbf{q} \quad (9)$$

Where $\mathbf{J}^+ = \mathbf{J}^T(\mathbf{J}\mathbf{J}^T)^{-1}$ is the Moore Penrose pseudo of \mathbf{J} . $\mathbf{N}(\mathbf{J})\mathbf{q}$ providing a vector in the null space of \mathbf{J} . Therefore, columns of $\mathbf{N}(\mathbf{J})$ should form a basis for the null space of \mathbf{J} and \mathbf{q} is an arbitrary vector. Note that the dimension of the null space is 3 in LCDR and hence $\mathbf{N}(\mathbf{J})$ has 3 columns. The second term in Eq. (9) is due to the fact that the number of cables is more than 6 and hence \mathbf{J} is not square. Physically, this term represents the pretension in the cables that balance each other and do not generate any external equivalent force or moment.

The stability analysis of the proposed robust control law in presence of unknown bounded disturbances is accomplished by using second method of Lyapunov. Thus, the Lyapunov candidate function is defined as

$$V(S) = \frac{1}{2} S^T S \quad (10)$$

Differentiating V with respect to time yields

$$(11)$$

Expanding Eq.(11) yields

$$\begin{aligned} \dot{V} &= \sum_{i=1}^6 s_i \left(\sum_{j=1}^6 |(\mathbf{M}^{-1})_{ij}| d_j - k_i \text{sign}(s_i) \right) \\ &\leq \sum_{i=1}^6 |s_i| \left(\sum_{j=1}^6 |(\mathbf{M}^{-1})_{ij}| f_j - k_i \right) \end{aligned}$$

$$\leq -\sum_{i=1}^6 \eta_i |s_i| \leq 0 \quad (12)$$

In other words, \dot{V} is strictly negative outside the sliding surface and consequently sliding condition is verified and stability and robustness of the proposed control law is ensured. It is obvious that η_i is a key parameter for convergence and robustness of proposed control law.

Note that the cable tensions given in Equation (9) involve infinite solutions for vector t . From these solutions only those that provide positive tension for all cables are acceptable. It is important to remember that, in general, there may be no such solution available. In that case the manipulator is not tensionable meaning that positive cable forces cannot be generated simultaneously in all cables. It is evident that, in such a case, the control will not be possible and the robot will collapse. It is assumed here that the mechanism is tensionable along the desired trajectory meaning that a tensile force solution exists for all cables.

It is also noteworthy that if Equation (9) has an acceptable solution for t , then it will not be unique since for instance any positive multiple of t is a solution too. This can be seen from the second term on the right hand side of Equation (9) which determines the pretension in the cables and is not unique. The best solution can be then selected to minimize a certain cost such as the mean value of the cable forces and certain constraints such the minimum and maximum allowed cable tensions [5]. As a result, the control law in case of the cable-driven mechanisms such as LCDR requires solving an optimization problem to decide the pretension of the cables. In this manipulator, the cable forces set by the controller are determined through the following optimization problem:

$$\begin{aligned} \text{Minimize:} & \quad f(t) = \frac{1}{9} \sum_{i=1}^9 t_i \\ \text{Linear Constraint:} & \quad Jt = (Jt)_{eq} - MK \text{ sign}(S) \\ \text{And:} & \quad t_{min} \leq t_i \leq t_{max} \quad \text{for } i = 1, \dots, 9 \end{aligned} \quad (13)$$

which can be solved using linear programming.

In this work, a gradient-based optimizer is used to solve the optimization problem (13). Gradient based optimization strategies iteratively search a minimum of a n-dimensional target function $f(t)$. Such optimizers use an initial estimate of the solution. Since a trajectory in workspace is continuous, the entries of the structure matrix, J , have small variations between two force distribution calculations. Thus, the initial estimate of the next force distribution calculation is very close to the last solution which results in short calculation times. Since a good initial estimate is available, the optimization is not very sensitive to the computation time. As a result, a gradient based optimizer was seen to provide a robust solution even in real-time applications. Such an optimizer was adapted and utilized under MATLAB to complete the controller design for LCDR.

6. Simulation

Simulation of the robot and the controller is performed using MATLAB. In this simulation scenario, the end-effector is initially at $(-0.1m, 0, -0.4m)$ and the desired end-effector trajectory is a circle in X-Y plane. The circle radius is $0.1 m$. Angle β is considered as the independent path parameter for the circle. End-effector starts and ends with zero velocity. We adopted the trajectory generation technique proposed in [13] which fits a smooth polynomial trajectory that satisfies the continuity conditions of velocity and acceleration at the via points. We require that angle β starts at zero and ends at 360° during the $5s$ motion; Also, we require that $\dot{\beta} = \ddot{\beta} = 0$ at the start and end of motion for the sake of smoothness. These conditions yield a fifth order polynomial for angle $\beta = 0.5026t^3 - 0.1508t^4 + 0.012t^5$ (rad). The associated trajectory, $\mathbf{X}_d(t)$, $\dot{\mathbf{X}}_d(t)$ and $\ddot{\mathbf{X}}_d(t)$ will be then calculated accordingly using β .

This simulation is done for two controller in presence of time variant disturbances; First for PID-Computed torque controller which proposed in [5] and second for proposed Sliding Mode Control via Double-Integrator Sliding Surface.

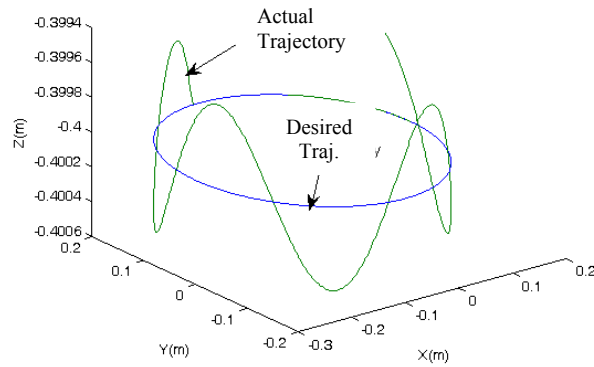


Fig. 3: Circle tracking simulation at the presence of time varying disturbance: PID-Computed Torque Control

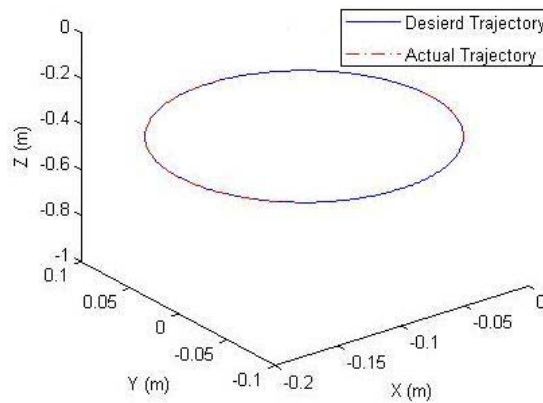


Fig. 4: Circle tracking simulation at the presence of time varying disturbance: Sliding Mode Control with PIID Sliding Surface

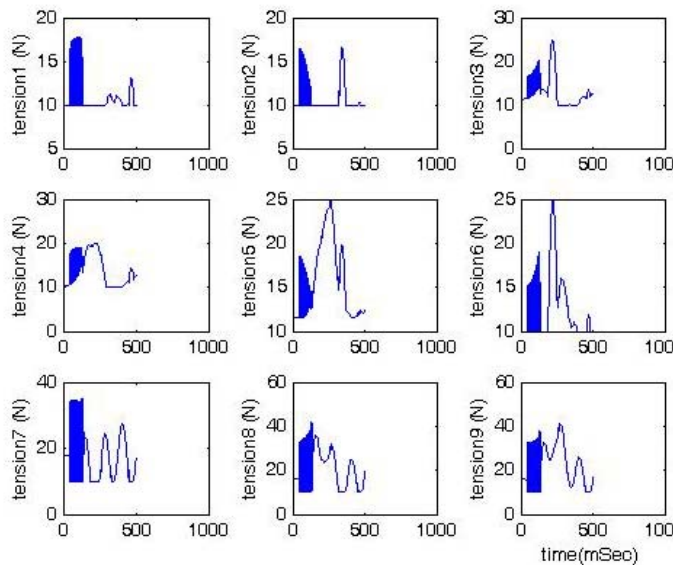


Fig. 5: Required cable tensions for circle tracking simulation at the presence of time-varying disturbances: Sliding Mode Control with PIID Sliding Surface

The simulation results are shown for the tracking problem with some time-varying disturbances on the external force applied to the end-effector. These disturbances are forces in the form of sinusoidal functions with magnitude of 10 N. It is important to note that the control law (9) only remains continuous prior to entering into the PIID sliding surface $S = 0$. It makes implementation so hard and impractical due to discontinuity of sign function at zero. Moreover, this discontinuity causes unwanted chattering phenomena which may excite the high frequency unmodeled dynamics. Thus, for continuous approximation of switching control law and alleviating chattering on terminal sliding surface, a saturation function is applied rather than sign function as follow

$$\text{sat}\left(\frac{\dot{\cdot}}{\varphi}\right) = \begin{cases} -1 & \text{if } \dot{\cdot} < -\varphi \\ \dot{\cdot} & \text{if } |\dot{\cdot}| \leq \varphi \\ 1 & \text{if } \dot{\cdot} > \varphi \end{cases} \quad (14)$$

where φ is called boundary layer thickness and is a positive constant.

In Figure 3, it can be seen that the disturbance causes error on the position in the PID-Computed torque control approach. However, the effectiveness and capability of proposed Sliding Mode Control with PIID Sliding Surface is shown in Figure 4. The closed-loop system not only tracks desired path against unknown uncertainties, but it also suppresses effectively steady state error regulation in comparison with PID-Computed torque and traditional sliding mode controllers. The positive cable tensions (control inputs) during the motion are also illustrated in Figure.5.

This indicates an acceptable performance of the trajectory tracker control for this robot by the proposed control in this paper.

7. Conclusion

This paper addresses the issue of modelling and robust control for the LCDR robot. In this manipulator, cable parallelograms are used to provide pure translational motion to the moving platform. The mechanism has potential for large scale manipulation and robotics in harsh environments. The robust control law is proposed based on sliding mode theory against inevitable model uncertainties and unknown disturbances. In addition, to eliminate the steady state error, two integral terms are added to sliding surface. Consequently, the proposed robust controller ensures positive cable tensions while acquired inequalities hold. Finally, numerical simulation results illustrate the effectiveness of the proposed scheme in comparison with PID-computed torque control which presented by author previously.

8. References

- [1] Saeed Behzadipour and Amir Khajepour, "A New Cable-Based Parallel Robot with Three Degrees of Freedom", *Multibody System Dynamics*, 2005, Vol.13, 371–383
- [2] Craig Kossowski and Leila Notash, "CAT4 (Cable Actuated Truss—4 Degrees of Freedom): A Novel 4 DOF Cable Actuated Parallel Manipulator", *Journal of Robotic Systems*, 2002, Vol. 19, 605–615
- [3] KeJun Ning, MingYang Zhao and Jie Liu, "A New Wire-Driven Three Degree-of-Freedom Parallel Manipulator", *Journal of Manufacturing Science and Engineering.*, 2006, Vol. 128, 816-819.
- [4] A.ALIKHANI, S. BEHZADIPOUR, S.A. SADOUGH VANINI, A. ALASTY, "Workspace Analysis of a Novel Three DoF Cable-driven Mechanism", *ASME Journal of Mechanisms and Robotics*, Vol. 1, No. 04, pp. 041005.1-041005.7, 2009.
- [5] A. Alikhani, S. Behzadipour, F. Ghahremani, A. Alasty, and S. A. Sadough Vanini, "Modeling, Control and Simulation of a new Large Scale Cable-driven Robot," *Proceeding of the ASME IDETC/CIE*, Cal., USA, 2009.
- [6] A. Alikhani and M. Vali, "Modeling and Robust Control of a New Large Scale Suspended Cable-driven Robot under Input Constraint" *Proceeding of the 8th International Conference on Ubiquitous Robots and Ambient Intelligence (URAI)*, Korea, 2011.
- [7] S. Tan, Y.M. Lai, and C.K. Tes, "Indirect Sliding Mode Control of Power Convertors Via Double Integral Sliding Surface" *IEEE Transactions on Electronics*, Vol.23, No.2, 600-611, 2008.
- [8]] R. Clavel, "Conception d'un robot parallèle rapide à 4 degrés de liberté," Ph.D Thesis, EPFL, Lausanne, Switzerland, 1991.
- [9] Robert L. Williams II, Paolo Gallina and Jigar Vadia, "Planar Translational Cable-Direct-Driven Robots", *Journal of Robotic Systems*, 2003, Vol. 20, 107–120
- [10] So-Ryeok Oh and Sunil K. Agrawal, "Cable Suspended Planar Robots With Redundant Cables:Controllers With Positive Tensions", *IEEE Transaction on Robotics*, 2005, Vol. 21, 457-465
- [11]J. J. slotine and W. Li, *Applied Nonlinear Control*, New Jersey: Prentice Hall, 1991.
- [12]C. Edwards and S. Spurgeon, *Sliding Mode Control: Theory and Application*, Taylor and Francis, 1998.
- [13]J.J. Craig, "Introduction to robotics: mechanics and control", Addison Wesley, Reading, MA, 1989.